PLOS ONE

Glutathione-Triggered Formation of a Fmoc-Protected Short Peptide-Based Supramolecular Hydrogel

Yang Shi[1], Jingyu Wang[1], Huaimin Wang[1], Yanhui Hu[2], Xuemei Chen[2], Zhimou Yang[1]*

1 State Key Laboratory of Medicinal Chemical Biology, Key Laboratory of Bioactive Materials, Ministry of Education, College of Life Sciences, and Collaborative Innovation Center of Chemical Science and Engineering (Tianjin), Nankai University, Tianjin, P. R. China, 2 School of Chemical and Materials Engineering, Hubei Institute of Technology, Huangshi, Hubei, P. R. China

Abstract

A biocompatible method of glutathione (GSH) catalyzed disulfide bond reduction was used to form Fmoc-short peptide-based supramolecular hydrogels. The hydrogels could form in both buffer solution and cell culture medium containing 10% of Fetal Bovine Serum (FBS) within minutes. The hydrogel was characterized by rheology, transmission electron microscopy, and fluorescence emission spectra. Their potential in three dimensional (3D) cell culture was evaluated and the results indicated that the gel with a low concentration of the peptide (0.1 wt%) was suitable for 3D cell culture of 3T3 cells. This study provides an alternative candidate of supramolecular hydrogel for 3D cell culture and cell delivery.

Data Availability: The authors confirm that all data underlying the findings are fully available without restriction. All relevant data are within the paper and its Supporting Information files.

Competing Interests: The authors have declared that no competing interests exist.

* Email: yangzm@nankai.edu.cn

Introduction

Supramolecular hydrogels of peptides have attracted extensive research interests in recent years due to the ease of design and synthesis, easy integration of bioactive ligands, and functionality [1–9]. They have shown big potential in three dimensional (3D) cell culture [10,11], controllable delivery of therapeutic agents [12–15], immune boosting [16], sensing [17–20], and regenerative medicine [21,22]. Among the reported peptide hydrogel systems, RADA16 and its derivatives [23,24], peptide amphiphiles [25,26], Q11 and its derivatives [27,28], FEK8 and its analogues [29,30], and those based on dipeptide of FF [31–35] are the most widely investigated. These peptide hydrogels are usually formed by ionic strength or pH change or organic solvent assistance. For the biomedical applications, methods to prepare peptide hydrogels in mild and biocompatible ways will be beneficial, which is actively explored recently [36]. Several biocompatible methodologies have been developed such as enzyme triggeration [37,38], photo-irradiation [39,40], redox control [41–43], and ligand-receptor interaction promotion [44]. Recently, Nilsson group had firstly developed a novel method of disulfide bond reduction to trigger a supramolecular hydrogel formation [45], which was followed by us to prepare short peptide-based hydrogels for cell culture and drug delivery [46]. We opted to applied this method to prepare hydrogels based on the Fmoc-FF and tested the possibility of the formed hydrogel in 3D cell culture, which was reported in this study.

Results and Discussion

Syntheses and rationale of the design

Hydrogels of Fmoc-FF was firstly reported by Ulijn and Gazit groups and the hydrogels have been applied for 3D cell culture [47,48]. The hydrogels were initially prepared by organic solvent (DMSO) assistance, and therefore a cell culture medium exchange procedure was needed to assist cell growth. Ulijn and co-workers then utilized the enzymatic reaction by a protease to prepare hydrogels based on Fmoc-FF [49].

We recently reported on a biocompatible triggeration of disulfide bond reduction catalyzed by glutathione (GSH) to form hydrogels for cell culture [50]. Due to the ease of synthesis of short peptides based on Fmoc-FF and the good properties of hydrogels of Fmoc-FF, we therefore attempted to further apply our GSH-triggered disulfide bond reduction method to prepare hydrogels based on Fmoc-FF. Similar to our previous report on the design of the pro-gelator of Nap-FFE-ss-EERGD [50], we designed and synthesized a possible pro-gelator of Fmoc-FFE-ss-EE, which was shown in Figure 1. We believed that the pro-gelator could be converted by GSH to a gelator of Fmoc-FFE-s, resulting in the hydrogel formation. Similar to the gels of Fmoc-FF, we imaged that the resulting hydrogel of Fmoc-FFE-s would also be suitable for 3D cell culture. We used Fmoc-CS reported in our previous study and Fmoc-amino acids with side chain protected for solid phase peptide synthesis to produce the design compound. The pure compound was obtained by reverse phase high performance liquid chromatography (HPLC, Figures S1 and S2 in File S1).
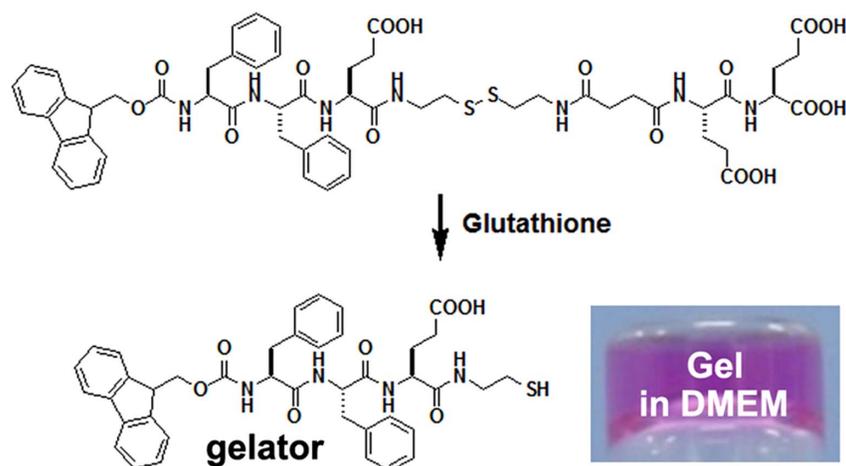
Figure 1. Chemical structure of the pro-gelator (Fmoc-FFE-ss-EE) and the resulting gelator (Fmoc-FFE-s) and an optical image of a gel formed by treating a DMEM solution containing 0.3 wt% of the pro-gelator with 4 equiv. of GSH.
doi:10.1371/journal.pone.0106968.g001

Hydrogel formation

The pro-gelator could be well solubilized in phosphate buffer saline (PBS, pH = 7.4) or cell culture Dul-becco's modified Eagle's medium (DMEM) medium with 10% of fetal bovine serum (FBS) at concentrations up to 5 wt% (50 mg/mL). We therefore tested its gelation ability by GSH conversion. As shown in Figure 1 (insert), a clear hydrogel could be obtained within 5 minutes after the addition of 4 equiv. of GSH to the DMEM solution with 10% of FBS of pro-gelator (0.5 wt%, 5 mg/mL). If using less amount of GSH, hydrogels could also form but it took a longer time. For example, for the PBS solution containing 0.5 wt% of the pro-gelator and 1 equiv. of GSH, it took about 50 minutes for the hydrogelation. The hydrogel was stable and would not change the clear appearance for more than six months at room temperature. The fast gelation kinetics, clear appearance, and good stability of the gel suggested its big possibility for 3D cell culture.

Rheology

We used a rheometer to monitor the gelation process and characterize the resulting hydrogel (Figures S3, S4, S5, S6 in File S1). As shown in Figure 2A, the hydrogel formed instantly after the addition of GSH to a DMEM solution containing 0.5 wt% of the pro-gelator, as demonstrating by the value of elasticity (G') dominating that of viscosity (G''). the mechanical property of the gel reached a balance after about 3,600 s, as indicating by the observation that both G' and G'' reached plateaus. We then performed dynamic frequency sweep to characterize the mechanical property of hydrogels formed at 3,600 s with different concentrations of pro-gelator. As shown in Figure 2B, gels with higher concentration of the peptide obviously possessed bigger G' values. For example, the G' value of gel from 0.3, 0.2, and 0.1 wt% of the pro-gelator was about 1800, 450, and 45 Pa, respectively. The gels showed weak frequency dependences at the frequency range from 0.1 to 100 rad/s and the G' value was at least 10 times bigger than its corresponding G'' value, suggesting the presence of high elastic networks in gels and the good mechanical property of the gels.

Cryo-transmission electron microscopy (cryo-TEM)

We then obtained a cryo-transmission electron microscopy (cryo-TEM) image to characterize the self-assembled nano-structures in the gel. As shown in Figure 3, we observed uniform
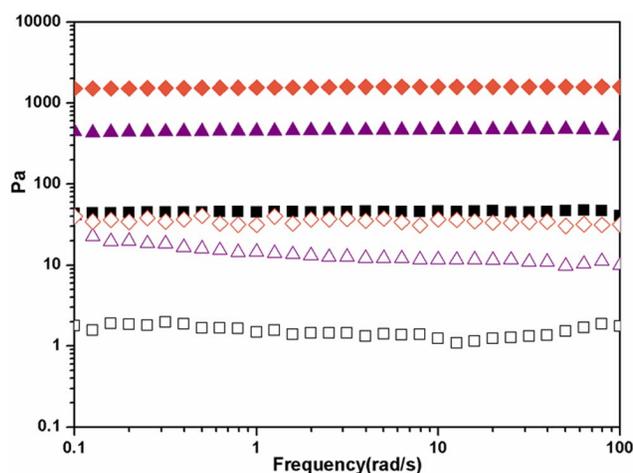

Figure 2. A representative rheological measurement with the mode of dynamic sweep at the frequency of 1 rad/s and the strain of 1% for a PBS solution containing 0.3 wt% of the pro-gelator and 4 equiv. of GSH (A) and rheological measurements with the mode of dynamic frequency sweep at the strain of 1% for gels from PBS solutions containing different concentrations of the pro-gelator (B) (filled symbols: G' and open symbols: G'', diamonds: 0.3 wt%, triangles: 0.2 wt%, and squares: 0.1 wt%).
doi:10.1371/journal.pone.0106968.g002

nanofibers with a width of about 8 nm in the gel. These fibers were helical with a left-handed helicity. They were longer than 2 µm and entangled with each other to form 3D networks for hydrogel formation. The examples of helical nanofibers in hydrogels were rare [51–55], and the helical nanofibers in this hydrogel might be useful as templates for the preparation of helical organic and in-organic nano-materials.

Emission spectra

In order to understand the aromatic arrangement of Fmoc in the nanofibers, we collected emission spectra of the PBS solution of pro-gelator and the resulting gel. As shown in Figure 4, the solution of pro-gelator exhibited a distinct peak centered at 328 nm, suggesting that the compound aggregated in the solution
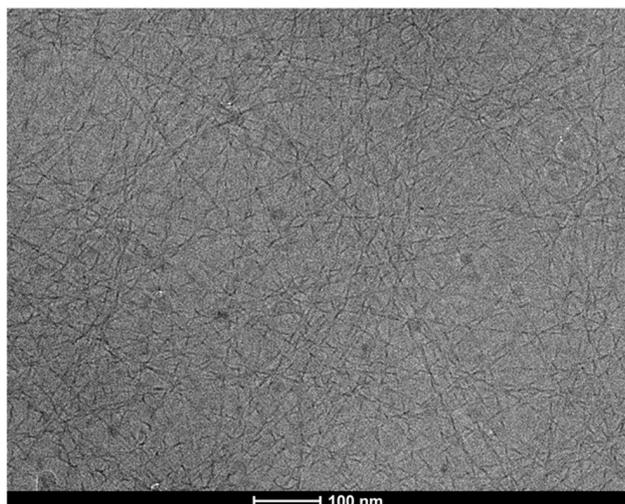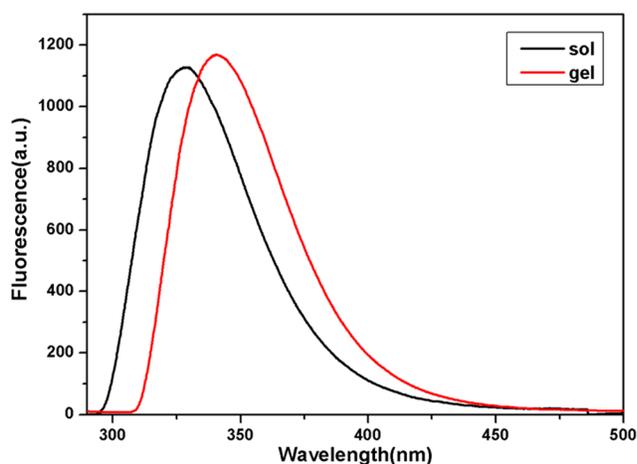
Figure 3. A cryo-transmission electron microscopy (cryo-TEM) image of the gel from a PBS solution containing 0.3 wt% of the pro-gelator with 4 equiv. of GSH.
doi:10.1371/journal.pone.0106968.g003

and the Fmoc groups favored the anti-parallel packing manner [35,56]. This peak shifted to 342 nm after the gel formation, suggesting that the Fmoc groups overlapped in the parallel manner in the gel [35,56]. The higher shoulder peak around 400 nm indicated that the Fmoc groups stacked more efficiently in the gel compared to those in the solution.

Cell culture

The gel from 0.3 wt% of the pro-gelator in PBS was stable for at least 5 days at 37°C in the incubator (Figure S7 in File S1), we therefore tested the possibility of resulting gels in 3D cell culture. We choose gels at different concentrations (0.3, 0.2, and 0.1 wt% of the pro-gelator) for 3D cell culture of NIH 3T3 cells. The cell-gel constructs could be obtained within 5 minutes after the addition of GSH. The volume of the gel was 50 µL in each well of the 96-well plate and the final cell density in the gel was 1,500,000/mL. 30 minutes after the formation of the cell-gel construct, we placed an additional 100 µL of DMEM supple-

mented with 10% of FBS on it. The CCK-8 assay was performed at day 1, 3, and 5 to determine the cell proliferation rate. Figure 5 showed that the 3T3 cells kept dividing in gels during the 5 culture days at the concentrations of 0.2 and 0.1 wt%, while they stopped proliferation in the gel at the concentration of 0.3 wt%. The gel from the solution of 0.1 wt% of the pro-gelator assisted the 3T3 cells the most efficiently within the three gels. The results in Figure S8 in File S1 indicated that the 3T3 cells at day 5 was homogeneously embedded in the gels formed by treating a DMEM solution containing 0.3 wt% of the pro-gelator with 4 equiv. of GSH. These observations indicated that gels with weaker mechanical properties were more suitable for the 3D culture of 3T3 cells, which was consistent with our previous results [46]. We hypothesized that cells in gels with weak mechanical properties could spread and divide more easily than those with strong mechanical properties.

After three days′ culture, we observed the cell morphology in gels by optical microscopy. As shown in Figure 6, 3T3 cells kept the round shape in the gel at 0.3 wt%. Most of cells spread well in the gel at 0.2 wt% and nearly total cells spread well in the gel at 0.1 wt%. These observations correlated well with the cell proliferation rate in Figure 5 and also suggested that gels with weaker mechanical property were more suitable for 3D cell culture of 3T3 cells. One shortcoming of our hydrogel is that we can not separate cells from gels post culture, and this problem may be addressed by developing other responsive supramolecular hydrogels.

Conclusions

In conclusion, we have demonstrated that the disulfide bond reduction strategy can be applied to prepare supramolecular hydrogels based on Fmoc-FF. the resulting hydrogels are optical transparent and stable, which are suitable for 3D cell culture. The results show that weak gels are suitable for 3D culture of 3T3 cells. The concentration of GSH was in the range of 1–10 mM in biological system, and the one we used to prepare hydrogels in this study is 0.86–2.59 mM, suggesting that our method is compatible for 3D cell encapsulation and culture. The good versatility and ease of handle will endow its good possibility for cell culture, cell delivery, and control release of bioactive molecules.
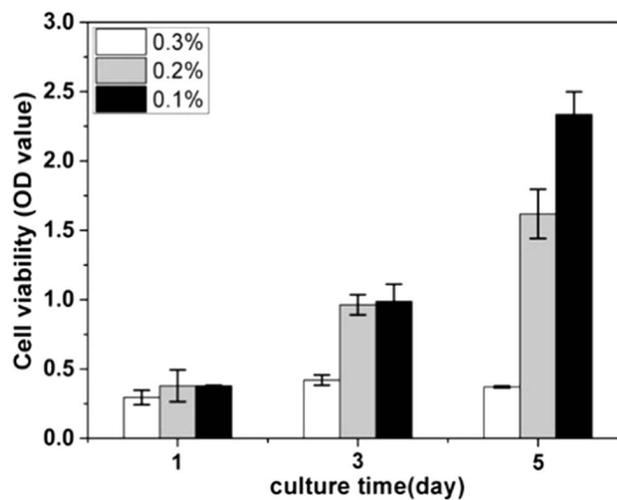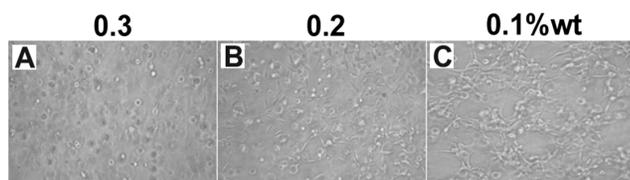

Figure 4. Emission spectra of PBS solution of the pro-gelator and the gel (excitation wavelength = 265 nm).
doi:10.1371/journal.pone.0106968.g004

Figure 5. Cell proliferation rate of 3T3 cells in gels at different concentrations determined by the CCK-8 assay.
doi:10.1371/journal.pone.0106968.g005

Figure 6. Optical images of cells at day 5 in gels at A) 0.3 wt%, B) 0.2 wt%, and C) 0.1 wt% (scale bars represent 10 µm).
doi:10.1371/journal.pone.0106968.g006

Materials and Methods

Materials and General methods

All the starting materials were obtained from G. L. Biochem. (Shanghai) or Sangon Biotech. (Shanghai). Commercially available reagents were used without further purification, unless noted otherwise. All other chemicals were reagent grade or better. PBS buffer (0.01 M, pH 7.4) was prepared with pills purchased from Sangon Biotech. Co., Ltd. (Shanghai, China). Ultrapure water (18.2 MΩ. cm) was used throughout the experiment. HepG2 human liver cancer cells were supplied by the Molecular Biology Laboratory of Anhui Medical University. High resolution ESI/MS spectra were obtained on a GCT premier mass spectrometer (Waters). HPLC analyses were performed on an Agilent 1200 HPLC system equipped with a G1322A pump and in-line diode array UV detector using a YMC-Pack ODS-AM column with CH_3OH (0.1% of TFA) and water (0.1% of TFA) as the eluent. ^{1}H-NMR spectra were obtained on a 300 MHz Bruker AV300. Cells were routinely cultured in Dul-becco's modified Eagle's medium (DMEM, Hycolon) supplemented with 10% fetal bovine serum at 37°C, 5% CO_2, and humid atmosphere.

Solid phase peptide synthesis

The peptide derivative was prepared by solid phase peptide synthesis (SPPS) using 2-chlorotrityl chloride resin and the corresponding N-Fmoc protected amino acids with side chains properly protected by a tert-butyl group. The first amino acid was loaded on the resin at the C-terminal with the loading efficiency about 0.6 mmol/g. 20% piperidine in anhydrous N,N′-dimethyl-formamide (DMF) was used during deprotection of Fmoc group. Then the next Fmoc protected amino acid was coupled to the free amino group using O-(benzotriazol-1-yl)-N,N,N′,N′-tetramethy-luroniumhexafluorophosphate (HBTU) as the coupling reagent and diisopropylethylamine (DIEA) as catalysis reagent. The growth of the peptide chain was according to the established Fmoc SPPS protocol. After the last amino acid was coupled, excessive reagents were removed by a single DMF wash for 5 min (5 mL per gram of resin), followed by 5 times DCM wash for 2 min (5 mL per gram of resin). The peptide was cleaved using 95% of trifluoroacetic acid (TFA) with 2.5% of trimethylsilane (TMS) and 2.5% of H_2O for 30 min. TFA was removed by a rotary-evaporator, then 20 mL per gram of resin of ice-cold diethylether was added. The resulting precipitate was dissolved in DMSO directly for HPLC separation with MeOH containing 0.1% of TFA and H_2O containing 0.1% TFA as eluents.

Hydrogel formation

The stock solution of pro-gelator was prepared at the concentration of 10 mg/mL (1 wt%), and the stock solution of GSH was prepared at the concentration of 10.8 mg/mL. The molar concentration of GSH stock solution was 4 times that of pro-gelator stock solution. During the preparation of the above two stock solutions, Na_2CO_3 was used to adjust the final pH value to be 7.4. Mixing two stock solutions with equal volume and with different amounts of PBS solution resulted in solutions containing different concentrations of the pro-gelator. Gels would form after being kept at room temperature (22–25°C) for within 5 minutes. The same procedure was used to prepare gels in DMEM solution, but replacing PBS solution with the DMEM solution.

CCK-8 assay

To quantify cell proliferation inside the cell-gel constructs, a CCK-8 assay was performed at a series of time points. A 3D Culture standard was made by encapsulating cells into hydrogels. Briefly, cells in culture medium with FBS, two stock solutions, and DMEM with FBS solution with different ratios were mixed together. The final cell density was 1,500,000/mL gel and the final concentration of the pro-gelator was 0.1, 0.2, or 0.3 wt%. The final solution was transferred to 96 well plates (50 µL per plate). After about half an hour, 100 µL of additional DMEM with 10% of FBS was added on the top of the gel. The plates were incubated in the 5% CO_2 incubator. To perform the CCK-8 assay, each cell-gel construct was washed with DMEM twice, and then incubated with 100 µL of 10% (v/v) CCK-8 in serum-free DMEM. The plates were then incubated in the 5% CO_2 incubator for 4 h at 37°C. The absorbance at 450 nm was determined using the microplate reader (MultiskaniMark, Bio-Rad, USA). The experiments were conducted for three times and SD was determined.

Supporting Information

File S1 **Synthesis and characterization, rheology, optical images, and Z-stacking scanning imaging in confocal microscope to show the homegeneous distribution of cells are included in File S1.**
(DOC)

Author Contributions

Conceived and designed the experiments: ZY XC. Performed the experiments: YS JW HW. Analyzed the data: YS YH XC ZY. Contributed to the writing of the manuscript: YS ZY. Did the syntheses, characterizations, and cell culture: YS. Did the cell culture: JW HW.

References

1. Collier JH, Rudra JS, Gasiorowski JZ, Jung JP (2010) Multi-component extracellular matrices based on peptide self-assembly. Chem Soc Rev 39: 3413–3424.
2. Gao Y, Zhao F, Wang Q, Zhang Y, Xu B (2010) Small peptide nanofibers as the matrices of molecular hydrogels for mimicking enzymes and enhancing the activity of enzymes. Chem Soc Rev 39: 3425–3433.
3. Wang H, Yang Z (2012) Short-peptide-based molecular hydrogels: novel gelation strategies and applications for tissue engineering and drug delivery. Nanoscale 4: 5259–5267.
4. Piepenbrock M-OM, Lloyd GO, Clarke N, Steed JW (2009) Metal-and anion-binding supramolecular gels. Chem Rev 110: 1960–2004.
5. Kumar DK, Steed JW (2014) Supramolecular gel phase crystallization: orthogonal self-assembly under non-equilibrium conditions. Chem Soc Rev 43: 2080–2088.
6. Steed JW (2010) Anion-tuned supramolecular gels: a natural evolution from urea supramolecular chemistry. Chem Soc Rev 39: 3686–3699.
7. Hirst AR, Escuder B, Miravet JF, Smith DK (2008) High-Tech Applications of Self-Assembling Supramolecular Nanostructured Gel-Phase Materials: From Regenerative Medicine to Electronic Devices. Angew Chem Int Ed 47: 8002–8018.
8. Boekhoven J, Poolman JM, Maity C, Li F, van der Mee L, et al. (2013) Catalytic control over supramolecular gel formation. Nature Chem 5: 433–437.

9. Minkenberg CB, Hendriksen WE, Li F, Mendes E, Eelkema R, et al. (2012) Dynamic covalent assembly of stimuli responsive vesicle gels. Chem Commun 48: 9837–9839.

10. Jayawarna V, Ali M, Jowitt TA, Miller AF, Saiani A, et al. (2006) Nanostructured Hydrogels for Three-Dimensional Cell Culture Through Self-Assembly of Fluorenylmethoxycarbonyl–Dipeptides. Adv Mater 18: 611–614.

11. Jung JP, Nagaraj AK, Fox EK, Rudra JS, Devgun JM, et al. (2009) Co-assembling peptides as defined matrices for endothelial cells. Biomaterials 30: 2400–2410.

12. Li X, Li J, Gao Y, Kuang Y, Shi J, et al. (2010) Molecular nanofibers of olsalazine form supramolecular hydrogels for reductive release of an anti-inflammatory agent. J Am Chem Soc 132: 17707–17709.

13. Wang H, Yang Z (2012) Molecular hydrogels of hydrophobic compounds: a novel self-delivery system for anti-cancer drugs. Soft Matter 8: 2344–2347.

14. Xu X-D, Liang L, Chen C-S, Lu B, Wang N-l, et al. (2010) Peptide hydrogel as an intraocular drug delivery system for inhibition of postoperative scarring formation. ACS Appl Mater Interf 2: 2663–2671.

15. Lin R, Cheetham AG, Zhang P, Lin Y-a, Cui H (2013) Supramolecular filaments containing a fixed 41% paclitaxel loading. Chem Commun 49: 4968–4970.

16. Rudra JS, Sun T, Bird KC, Daniels MD, Gasiorowski JZ, et al. (2012) Modulating adaptive immune responses to peptide self-assemblies. ACS Nano 6: 1557–1564.

17. Ikeda M, Yoshii T, Matsui T, Tanida T, Komatsu H, et al. (2011) Montmorillonite− supramolecular hydrogel hybrid for fluorocolorimetric sensing of polyamines. J Am Chem Soc 133: 1670–1673.

18. Cai Y, Shi Y, Wang H, Wang J, Ding D, et al. (2014) Environment-sensitive fluorescent supramolecular nanofibers for imaging applications. Anal Chem 86: 2193–2199.

19. Xu XD, Lin BB, Feng J, Wang Y, Cheng SX, et al. (2012) Biological Glucose Metabolism Regulated Peptide Self-Assembly as a Simple Visual Biosensor for Glucose Detection. Macromol Rapid Comm 33: 426–431.

20. Bremmer SC, Chen J, McNeil AJ, Soellner MB (2012) A general method for detecting protease activity via gelation and its application to artificial clotting. Chem Commun 48: 5482–5484.

21. Shah RN, Shah NA, Lim MMDR, Hsieh C, Nuber G, et al. (2010) Supramolecular design of self-assembling nanofibers for cartilage regeneration. Proc Natl Acad Sci U S A 107: 3293–3298.

22. Gelain F, Unsworth LD, Zhang S (2010) Slow and sustained release of active cytokines from self-assembling peptide scaffolds. J Control Release 145: 231–239.

23. Yokoi H, Kinoshita T, Zhang S (2005) Dynamic reassembly of peptide RADA16 nanofiber scaffold. Proc Natl Acad Sci U S A 102: 8414–8419.

24. Zhao Y, Yokoi H, Tanaka M, Kinoshita T, Tan T (2008) Self-assembled pH-responsive hydrogels composed of the RATEA16 peptide. Biomacromolecules 9: 1511–1518.

25. Beniash E, Hartgerink JD, Storrie H, Stendahl JC, Stupp SI (2005) Self-assembling peptide amphiphile nanofiber matrices for cell entrapment. Acta Biomaterialia 1: 387–397.

26. Behanna HA, Donners JJ, Gordon AC, Stupp SI (2005) Coassembly of amphiphiles with opposite peptide polarities into nanofibers. J Am Chem Soc 127: 1193–1200.

27. Collier JH, Messersmith PB (2003) Enzymatic modification of self-assembled peptide structures with tissue transglutaminase. Bioconjugate Chem 14: 748–755.

28. Collier JH, Messersmith PB (2004) Self-Assembling Polymer–Peptide Conjugates: Nanostructural Tailoring. Adv Mater 16: 907–910.

29. Marini DM, Hwang W, Lauffenburger DA, Zhang S, Kamm RD (2002) Left-handed helical ribbon intermediates in the self-assembly of a β-sheet peptide. Nano Lett 2: 295–299.

30. Du X, Wu Z, Long J, Wang L (2013) Growth stimulation of bacterium Delftia by a peptide hydrogel. RSC Adv 3: 18259.

31. Kuang Y, Gao Y, Xu B (2011) Supramolecular hydrogelators of N-terminated dipeptides selectively inhibit cancer cells. Chem Commun 47: 12625–12627.

32. Zheng W, Gao J, Song L, Chen C, Guan D, et al. (2012) Surface-Induced Hydrogelation Inhibits Platelet Aggregation. J Am Chem Soc 135: 266–271.

33. Wang Z, Wang H, Zheng W, Zhang J, Zhao Q, et al. (2011) Highly stable surface modifications of poly (3-caprolactone)(PCL) films by molecular self-assembly to promote cells adhesion and proliferation. Chem Commun 47: 8901–8903.

34. Kuang Y, Xu B (2013) Disruption of the dynamics of microtubules and selective inhibition of glioblastoma cells by nanofibers of small hydrophobic molecules. Angew Chem Int Ed 52: 6944–6948.

35. Smith AM, Williams RJ, Tang C, Coppo P, Collins RF, et al. (2008) Fmoc-Diphenylalanine Self Assembles to a Hydrogel via a Novel Architecture Based on π–π Interlocked β-Sheets. Adv Mater 20: 37–41.

36. Wang H, Yang Z, Adams DJ (2012) Controlling peptidebased hydrogelation. Mater Today 15: 500–507.

37. Yang Z, Liang G, Xu B (2008) Enzymatic hydrogelation of small molecules. Acc Chem Res 41: 315–326.

38. Debnath S, Roy S, Ulijn RV (2013) Peptide Nanofibers with Dynamic Instability through Nonequilibrium Biocatalytic Assembly. J Am Chem Soc 135: 16789–16792.

39. Qiu Z, Yu H, Li J, Wang Y, Zhang Y (2009) Spiropyran-linked dipeptide forms supramolecular hydrogel with dual responses to light and to ligand–receptor interaction. Chem Commun: 3342–3344.

40. He M, Li J, Tan S, Wang R, Zhang Y (2013) Photodegradable Supramolecular Hydrogels with Fluorescence Turn-On Reporter for Photomodulation of Cellular Microenvironments. J Am Chem Soc 135: 18718–18781.

41. Zhang Y, Zhang B, Kuang Y, Gao Y, Shi J, et al. (2013) A Redox Responsive, Fluorescent Supramolecular Metallohydrogel Consists of Nanofibers with Single-Molecule Width. J Am Chem Soc 135: 5008–5011.

42. Miao X, Cao W, Zheng W, Wang J, Zhang X, et al. (2013) Switchable Catalytic Activity: Selenium-Containing Peptides with Redox-Controllable Self-Assembly Properties. Angew Chem Int Ed 52: 7781–7785.

43. Sun Z, Li Z, He Y, Shen R, Deng L, et al. (2013) Ferrocenoyl Phenylalanine: A New Strategy Toward Supramolecular Hydrogels with Multistimuli Responsive Properties. J Am Chem Soc 135: 13379–13386.

44. Zhang X, Chu X, Wang L, Wang H, Liang G, et al. (2012) Rational Design of a Tetrameric Protein to Enhance Interactions between Self-Assembled Fibers Gives Molecular Hydrogels. Angew Chem Int Ed 124: 4464–4468.

45. Bowerman CJ, Nilsson BL (2010) A reductive trigger for peptide self-assembly and hydrogelation. J Am Chem Soc 132: 9526–9527.

46. Lv L, Liu H, Chen X, Yang Z (2013) Glutathione-triggered formation of molecular hydrogels for 3D cell culture. Colloid Surface B 108: 352–357.

47. Jayawarna V, Ali M, Jowitt TA, Miller AF, Saiani A, et al. (2006) Nanostructured Hydrogels for Three-Dimensional Cell Culture Through Self-Assembly of Fluorenylmethoxycarbonyl–Dipeptides. Adv Mater 18: 611–614.

48. Mahler A, Reches M, Rechter M, Cohen S, Gazit E (2006) Rigid, Self-Assembled Hydrogel Composed of a Modified Aromatic Dipeptide. Adv Mater 18: 1365–1370.

49. Toledano S, Williams RJ, Jayawarna V, Ulijn RV (2006) Enzyme-triggered self-assembly of peptide hydrogels via reversed hydrolysis. J Am Chem Soc 128: 1070–1071.

50. Ren C, Song Z, Zheng W, Chen X, Wang L, et al. (2011) Disulfide bond as a cleavable linker for molecular self-assembly and hydrogelation. Chem Commun 47: 1619–1621.

51. Fu Y, Li B, Huang Z, Li Y, Yang Y (2013) Terminal is important for the helicity of the self-assemblies of dipeptides derived from alanine. Langmuir 29: 6013–6017.

52. Yang Y, Suzuki M, Owa S, Shirai H, Hanabusa K (2007) Control of mesoporous silica nanostructures and pore-architectures using a thickener and a gelator. J Am Chem Soc 129: 581–587.

53. Duan P, Qin L, Zhu X, Liu M (2011) Hierarchical Self-Assembly of Amphiphilic Peptide Dendrons: Evolution of Diverse Chiral Nanostructures Through Hydrogel Formation Over a Wide pH Range. Chem-Eur J 17: 6389–6395.

54. Wang T, Jiang J, Liu Y, Li Z, Liu M (2010) Hierarchical self-assembly of bolaamphiphiles with a hybrid spacer and L-glutamic acid headgroup: pH-and surface-triggered hydrogels, vesicles, nanofibers, and nanotubes. Langmuir 26: 18694–18700.

55. Cao H, Zhu X, Liu M (2013) Self-Assembly of Racemic Alanine Derivatives: Unexpected Chiral Twist and Enhanced Capacity for the Discrimination of Chiral Species. Angew Chem Int Ed 52: 4122–4126.

56. Channon KJ, Devlin GL, Magennis SW, Finlayson CE, Tickler AK, et al. (2008) Modification of fluorophore photophysics through peptide-driven self-assembly. J Am Chem Soc 130: 5487–5491.